

Magnetic Capsule for Stable Collection of Large GI Tract Microbiome Samples

Taeyoung Lee and Eric Diller, *Senior Member, IEEE*

Abstract— The gut microbiome is an important indicator and determinant of human health, but current methods to sample intestinal contents are insufficient. Robotic sampling capsules hold the unique potential to sample contents in a non-invasive manner for safe study and diagnosis, but suffer from low sampling volume and poor sealing robustness. We introduce a new tetherless magnetically actuated capsule designed for noninvasive sampling of GI liquid digesta for study. The design uniquely maximizes sampling volume efficiency, utilizing 52% of its space (290 mg) for the sample, compared to roughly 10% in previous magnetic hinge designs. Controlled by low strength magnetic fields, the capsule operates without onboard control circuits, enabling sampling anywhere along the GI tract. Strong magnetic sealing forces (2.8 N) prevent leakage or contamination of the sample. The capsule's compact size (8 mm diameter, 11 mm length) is similar to existing FDA approved GI capsules, allowing safe transit through the body. It features a wide opening angle of 144 degrees, and stays closed for low fields to avoid accidental opening (the hinge snaps open to 83% of its maximum opening angle within an increment of just 2 mT of the last closed point). The capsule's robust design withstands GI pressures (roughly 10 kPa).

I. INTRODUCTION

The role of the gut microbiome in human health is increasingly recognized due to its association with a number of human diseases [1], [2], [3]. Understanding the interactions between the gut microbiome and the host immune system is clinically important, and will potentially lead to developing new therapeutic strategies for associated human diseases [3]. Currently available diagnostic methods for gut-related diseases involve fecal microbiota samples, endoscopic biopsy, x-ray, or surgery, but these methods are highly invasive, complex, require a prolonged procedural time, expensive, and yield inaccurate test results if only fecal material is sampled which is not representative of the entire intestinal tract microbiome [4], [2]. The challenge is thus the non-invasive retrieval of pristine physical intestinal content samples for study and diagnosis from an arbitrary location in the gastrointestinal (GI) tract [5]. Several designs have been proposed for controllable small-scale robotic capsule robots for gut microbiome sampling as a solution to this challenge. Designs include locomotion and sampling mechanisms powered by motorized tools, acoustical methods, chemical fuels, stimuli-responsive material assistance, electric circuits, and magnetic control [6], [7]. Ingestible pill-sized capsules will allow minimally-invasive sampling of the GI tract [8].

Department of Mechanical and Industrial Engineering, University of Toronto, 5 King's College Rd, Toronto, ON, M5S 3G8, Canada (e-mail: taeyoungty.lee@mail.utoronto.ca, ediller@mie.utoronto.ca).

Current ingestible capsules can collect tissue biopsies [9], deliver drugs [6], and sample liquids [5]. However, existing sampling capsules face significant limitations including the inability to maintain stable latching of open/close states, sample quantities which are too small for analysis, and contamination issues due to inherent design constraints [5]. Passive chemical-aided capsules, once activated, are irreversible, complicating the control of undesired operations [10], [11], [12]. Fluid sampling capsules encounter challenges in effective performance and precise control, often requiring complex electronic and mechanical components that reduce the available sampling reservoir volume [13], [14], [15], [16]. Lastly, sampling chambers can leak if unpredictable and strong peristalsis motion in the stomach and intestines triggers accidental opening. The limitations are summarized in Table I.

This paper follows a prior magnetically-actuated sampling capsule (BCMAC) from our group [5] which opens with a hinge to expose the internal sample collection chamber, and relies on magnetic field for both locomotion (low strength field) and chamber opening (using high strength field). The actuating field can be generated by a large external permanent magnet or electromagnetic coil system. The BCMAC is simple in operation and design, but is susceptible to accidental chamber opening during locomotion. The capsule also suffers from poor sampling efficiency of 7.5%, and a small reservoir of 42 mm³ with a hinge opening of 8 degrees [5]. Therefore, there is need for an improved magnetic capsule that can actively collect samples with a reliable opening/sealing mechanism. We define the metric of sampling efficiency as the ratio of the collected sample volume to the total chamber volume [17], [18].

We propose the novel tetherless magnetically actuated snap-open capsule (SOMAC) as seen in Fig. 1, a capsule offering higher volume ratio of 52% and increased sampling reservoir volume of 290 mm³ due to a larger hinge opening angle (144 degrees) and a wider exposed surface area (88 mm²) than our previous design. SOMAC features a re-considered magnet and hinge placement, enabling unambiguous chamber snap-open behavior at lower magnetic fields (<10 mT), and potential for smaller size (8 mm outer diameter and 11 mm length). The design also minimizes the risk of sample contamination by achieving a higher sealing force (2.8 N versus 0.7 N for [5]) and unambiguous snap-open design through the optimized size, orientation, and placement of small internal magnets (type N50; 4 mm long, 2 mm wide, 4 mm thick; magnetized through the thickness). These improvements aim to provide more reliable and effective sampling capabilities in various environmental conditions. This paper introduces the design concepts and

TABLE I. COMPARISON OF ACTIVE AND PASSIVE SAMPLING CAPSULES, HIGHLIGHTING THE HIGH VOLUME RATIO OF THE PROPOSED CAPSULE DESIGN

COMPARISON OF SAMPLING DEVICES TO COLLECT GUT MICROBIOME SAMPLES				
Type	Sampling Mechanism (Actuation Method) [Ref.]	Overall Size Dia x Length (mm x mm)	Maximum Sampling Volume (μL)	Sampling Volume as Percentage of Capsule Size
Active	Hinge Door (SMA spring) [16]	12 x 45	128	2.5%
	Pump (Motorized pump) [14]	10.2 x 30	262	10%
	Hinge Door (Magnetic) [5]	8 x 11	42	7.5%
	Micropump (Magnetic) [2]	11 x 26	15*3	1.8%
	Hinge Door (Magnetic) SOMAC This work	8 x 11	290	52%
Passive	Hydrogel Swelling (Hydrogel) [4]	8 x 19	31	3.2%
	Hydrogel Swelling (Hydrogel) [10]	9 x 15	282.7	29%
	Foam swelling (Porous Foam) [11], [12]	9 x 26	200	12%

SMA = Shape Memory Alloy

sampling mechanisms of the SOMAC, explains a mathematical model of its actuation processes, and proves the sampling capsule's actuation abilities in experiments including *in vitro*, and *ex vivo* sampling scenarios.

II. CAPSULE DESIGN

A. Selecting a Template (Heading 2)

The SOMAC capsule is designed to navigate the limited space of the human GI tract while maximizing sampling volume efficiency. Capsule sizes of 11 mm in diameter and 26 mm in length [5] match that of FDA approved capsule endoscopes, so we limit the capsule to that overall size which must include internal actuation and sample chamber. Here we use the metric of sampling efficiency to mean the ratio of the collected sample volume to the total chamber volume [17], [18], expressing the effectiveness of filling the available chamber with liquid digesta containing microbiome sample. A large chamber with high sampling efficiency is critical for diagnostic and microbiome study purposes, as it enables comprehensive analysis of GI microbiome and their interactions with the host immune system by 16S RNA survey or other methods [5]. Sampling capsules endure gastric pressures around 10 kPa during GI transit [19] so the design should not crush or distort under such forces. Particularly, since the area where the capsule opens and closes is the most vulnerable part to leakage and contamination, the capsule should be reinforced by sufficient sealing forces and an elastic seal rim made of low-stiffness material. To enable simple tetherless operation using an external magnet without an imaging system, the magnetically controlled capsule should actuate under fields as low as around 15 mT which can be generated at the distance within a human torso [5].

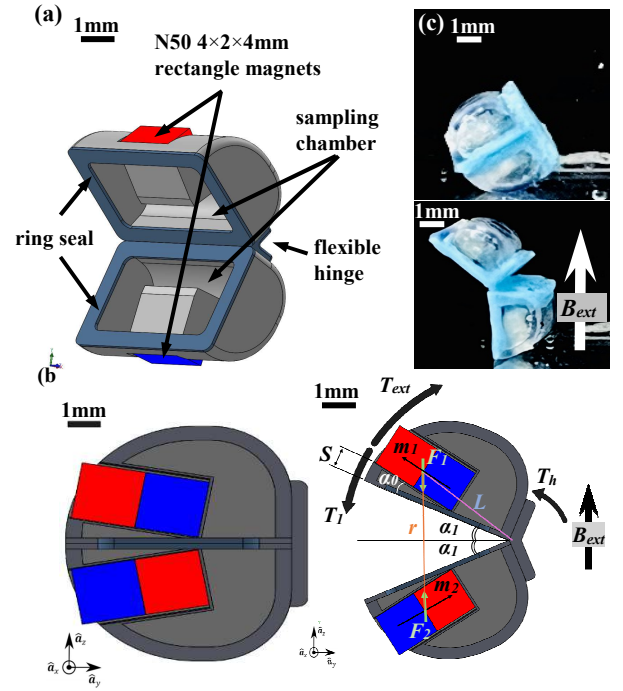


Fig. 1. Design of the novel remotely controlled magnetically actuated snap-open capsule (SOMAC). (a) Isometric view of SOMAC, highlighting the major components. Each half of the symmetrical sides contains a sampling chamber, internal magnet, sealing mechanism, and hinge. (b) SOMAC in two actuation states (closed to open for sampling) with a schematic of the applied torques and angles. The two internal permanent magnets (m_1 and m_2) are slanted at a 10° angle (α_0), creating net magnetization when the capsule is closed. The applied magnetic torques and inter-magnet forces are depicted on the top and bottom halves of the SOMAC in a free-body diagram. (c) Photographs of SOMAC in both the closed and open states.

All components of the capsule must be non-toxic and unaffected by the low-pH conditions of the GI tract, as low as 1.5 in the stomach [20]. The affordable and scalable capsule design should be simple for easy fabrication and repeat assembly, reducing complexity processes to make a fully functional capsule device.

B. Capsule Actuation Mechanism

SOMAC operates in the normally-closed configuration, and opens in response to a larger magnetic field for sample collection. The embedded orientation of the two internal magnets is opposite, which results in an attractive force between the magnets to keep SOMAC closed and tightly sealed until sufficient magnetic torque from the externally-generated magnetic field is exerted to overcome the sealing attraction (see Fig. 1b). To align the capsule prior to activation, the magnets are tilted slightly by angle α_0 which induces a small net magnetic moment which serves to align the entire capsule with the applied field, at which point the field can be increased for opening, as in reference [5] (see Fig. 1b).

As a result of this magnet location, the sampling capsule will open abruptly under magnetic fields and latch the opening angle open for optimal filling of the chamber. Subsequently, when the applied magnetic field is removed, SOMAC automatically returns to the initial closed state due to its closing torque from the internal magnets' attraction as well as the restoring torque from the flexible hinge (respectively, T_l ,

T_{Fi} , T_h). The opposite orientations between the internal magnets play a critical role in creating an inter-magnetic attractive force in the SOMAC design. The attraction force can keep the capsule closed under the influence of various external and internal forces and torques, and can improve sealing safety, resulting in superior prevention of leakage and cross contamination. Although the smaller volume of internal magnets compared to the previous design generates weaker magnetic torques from the externally applied field, the closer inter-magnet distance creates much stronger magnetic strength. This is because the magnetic force is directly proportional to volume and inversely proportional to distance squared [5].

C. Mathematical Model

Magnetic torques and forces play a key role in understanding the capsule's actuation system. A mathematical model which captures the opening/closing behavior is required to optimize the position of internal magnets and the maximum opening angles along an external magnetic field. To estimate the capsule design with the successful functionality (closed→opened (sampling)), magnetic torque and force should be analyzed. For the opening mechanism, an applied magnetic field (B_{ext}) generates an external torque (T_{ext}) on each internal magnet of magnetic moment m_1 and m_2 , which acts to bring each magnet's magnetization direction into alignment with the field (see Fig. 1b). The effect of the applied field is thus to create an opposite magnetic torque on each capsule magnet, which opens the capsule. This external torque should overcome the sum of closing torque from the opposite oriented internal magnets and restoring torques from the flexible hinge (T_l , T_{Fi} , T_h) to open the capsule. The sum of torques on one side of the capsule is thus

$$T_l + L \times F_l + T_h + m_i \times B_{ext} = 0. \quad (1)$$

A dipole field model can be used to calculate the field and field gradient generated on an internal magnet due to the other magnet's field as

$$\mathbf{T}_1 = -\frac{\mu_0 \cdot m^2}{8\pi r^3} \sin(2\alpha) \hat{\mathbf{a}}_x \text{ and} \quad (2)$$

$$\mathbf{F}_1 = \frac{3\mu_0 \cdot m^2}{4\pi r^4} (-1 - \sin^2(\alpha)) \hat{\mathbf{a}}_y, \quad (3)$$

where μ_0 is the magnetic permeability of free space (value of $1.257 \times 10^{-6} \frac{H}{m}$), m is the magnetic moment of internal permanent magnets $m = m_1 = m_2$ (value of 0.0369 Am^2), r is the vector distance between the center of mass (COMs) of the two internal magnets, α is sum of α_1 (half of the opening angle) and α_0 (a small offset angle and the value of 10°) and $\hat{\mathbf{a}}_x$ and $\hat{\mathbf{a}}_y$ are the unit vectors of the coordinate system attached to the capsule (see Fig. 1b) [5].

Combining equations (1-3), the torque balance can be expressed as

$$\frac{\mu_0 \cdot m^2}{8\pi r^3} \sin(2\alpha) \hat{\mathbf{a}}_x + \frac{3\mu_0 \cdot L \cdot m^2}{4\pi r^4} (1 + \sin^2(\alpha)) \cos(\alpha' + \alpha_1) \hat{\mathbf{a}}_x + \left(\frac{3EI \tan(\alpha_1)}{l'} \right) \hat{\mathbf{a}}_x - m B_{ext} \cos(\alpha) \hat{\mathbf{a}}_x = 0, \quad (4)$$

where L is the position vector from the hinge COM to internal magnet COM, α' is the angle between the plane intersecting both halves of the capsule and the plane passing through the COMs of the hinge and internal magnet across the capsule

diagonally. The hinge torque (T_h) is calculated with a rectangular cantilever beam model using the Euler–Bernoulli theory, where l' is the length of the hinge, E is the Young's modulus measured experimentally by a tensile test, and I is the second moment of inertia of the cross-section area of the hinge. The hinge geometrical dimensions (length and thickness) play important roles in equation (4) as studied in [5]. The optimized position and size of internal magnets and the flexible hinge and the maximum opening angles along an external magnetic field will be explored using this model. Our capsule design was created through a process of brute force search by choosing the magnet's location and size and flexible hinge, resulting in strong sealing force and the ability to snap-opening behavior at lower magnetic fields. The unambiguous opening angle and sealing forces are calculated and experimentally verified in Section IV.

III. FABRICATION

A. Capsule Fabrication

In Fig. 1, the capsule body components (8 mm outer diameter and 11 mm length, with a high-volume sampling chamber capable of holding up to 290 mm^3 and a surface area of 88 mm^2) were prepared using SolidWorks 2020 (SolidWorks Corporation., Dassault Systèmes) and 3D printed with a standard clear V4 resin using a Form3 3D printer (FormLabs Inc.). Clear V4 resin is a rigid material and the 64 MPa of ultimate tensile strength can protect the thin wall thickness from any deformation or damage under harsh conditions such as irregular motion and agitation [21].

B. Sealing and Hinge Mechanism Fabrication

The sealing and hinge fabrication process were similar, but they were made in different molds (sealing mold and hinge mold). The fabricating process entails two primary procedures: material fabrication and compression molding. The customized molds for the rectangle-ring shaped sealing rim and hinge part were prepared using SolidWorks 2020 and 3D printed using a Form3 printer. To optimize the material properties of the selected Mold Star 30 silicone rubber for this design, different weight percentages of silicone rubber Part A and Part B (1:1, 1:0.8, 1:0.6, 1:0.4, 1:0.2) were fabricated and tested. Based on the material characterization, 20 wt% Part B was chosen as the proposed material offered desired material properties on SOMAC design [22]. The material (20 wt% Part B) was compressed on the molds to force it into contact with all mold areas and cured based on the fabrication procedure [22] (See Fig. 2). After the curing process, the cured materials were demolded and waited for assembly procedure or material property test.

C. Final Assembly

When all capsule components were ready, $4 \times 2 \times 4 \text{ mm}$ of internal magnets (type N50; 4 mm long, 2 mm wide, 4 mm thick; magnetized through the thickness) were installed to desired position and orientation on each side of the half

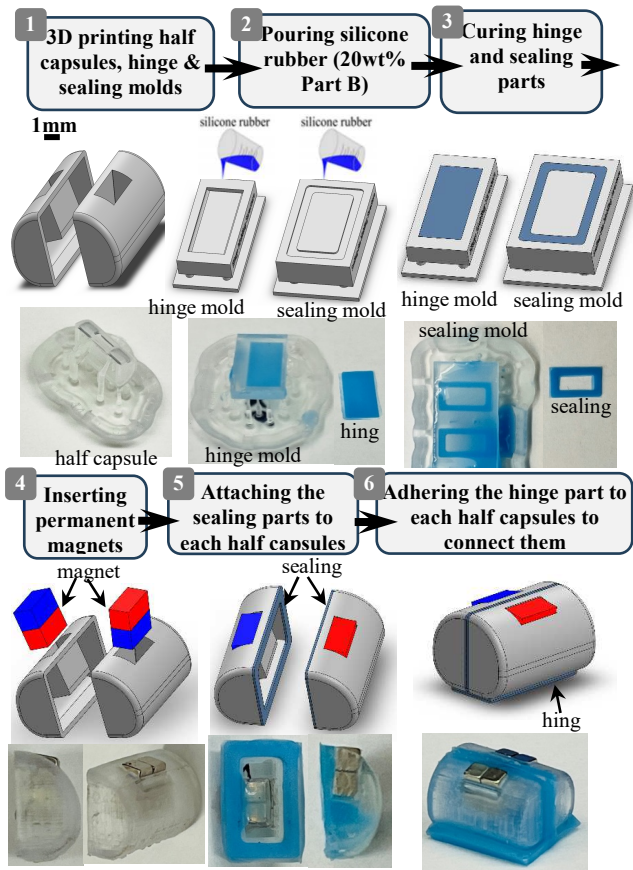


Fig. 2. Schematic and photographs of the fabrication process and assembly steps. (1) Development of half capsules and molding structures. (2) Pouring silicone rubber (20 wt% Part B). (3) Curing the sealing and hinge components. (4) Installation of internal magnets. (5) Attaching the rectangular ring seal to each half of the capsule. (6) Adhering the hinge component to connect the two halves of the capsule.

capsule. The rectangle-ring seal was attached to around the opening surfaces on each half capsule. The optimized size of the flexible hinge was adhered to the bottom of the two half capsules to connect to each other. After finishing the assembly steps and removing sharp edges for patient safety during GI transit, the SOMAC is formed and ready for use.

The simple fabrication of magnetically operated capsule design can reduce complex processes to make a full functionality. This can eliminate the need for cumbersome tethers or control circuits and omit extra steps such as chemical affinity coating or hydrophilic coating to increase the sampling amount due to high sampling efficiency from bigger opening angles, increased surface area, and higher sampling volume.

IV. EXPERIMENTS

A. Model Validation for Optimized Design

This section investigates the minimum magnetic field required to achieve clear snap-opening behavior in several capsule designs, ultimately optimizing the design for actuation using an 8-coil electromagnetic system available in our lab. The goal was to optimize a capsule design that could

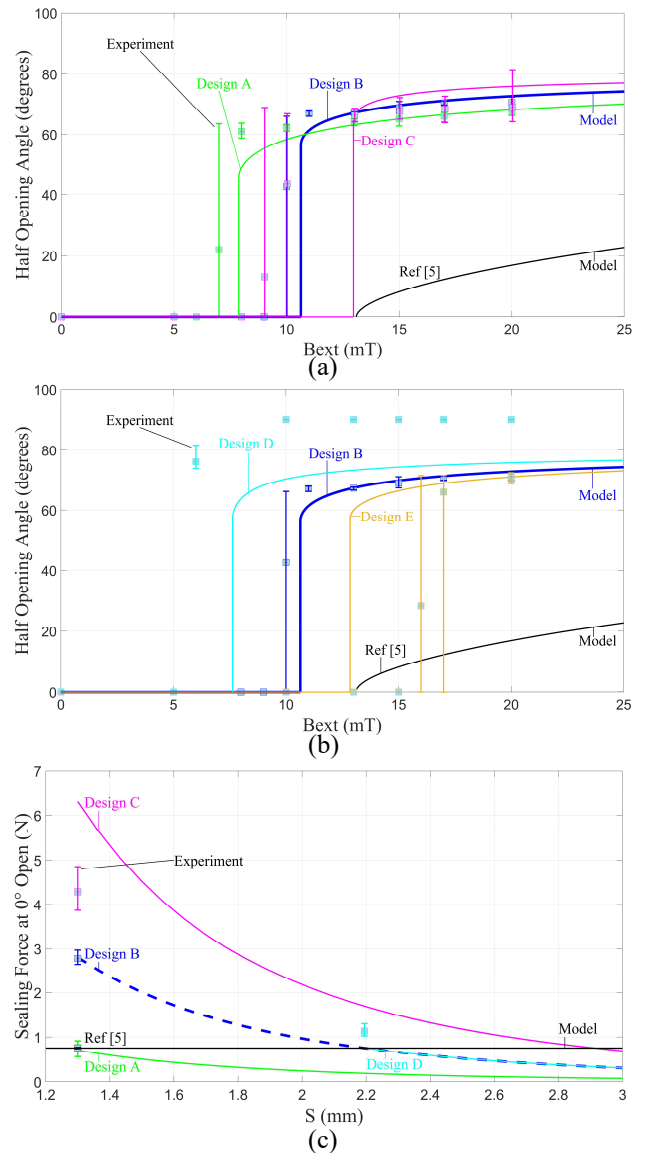


Fig. 3. Calculated half snap-opening angle (α_1) of the SOMAC designs along external magnetic field (B_{ext}) using the interaction torque equation (1). (a) Three different internal magnet sizes are compared: Design A ($2 \times 2 \times 4$ mm), Design B ($4 \times 2 \times 4$ mm), and Design C ($6 \times 2 \times 4$ mm). (b) Three different distances between internal magnets are compared: Design D (farthest distance, $S=2.20$ mm), Design B (optimized distance, $S=1.30$ mm), and Design E (closest distance, $S=0.78$ mm). (c) Calculated SOMAC sealing force as a function of distance S (the position vector originating from the opening edge, the farthest from the hinge, of the half capsule to the outer edge, the closest to the opening edge, of the internal magnet) using a dipole field gradient model shown in equation (3). Four different designs are compared: Design A, B, C, and D. All results are compared with experimental measurements ($n = 5$ capsules, each tested five times for all data points; error bars represent standard deviation) and BCMAC [5].

open unambiguously with at a certain low external magnetic field for sample collection. To achieve this, five capsule designs were evaluated by varying the size and position of internal magnets for comprehensive understanding of trade-off among multiple optimization objectives. Three different magnet sizes were tested: Design A ($2 \times 2 \times 4$ mm), Design B ($4 \times 2 \times 4$ mm), and Design C ($6 \times 2 \times 4$ mm). Additionally, the effect of internal magnet positioning was assessed in Design D (farthest distance at 2.20 mm), Design B (optimized distance

at 1.30 mm), and Design E (closest distance at 0.78 mm). The capsules ($n=5$ capsules on each design and tested them five times) were subjected to increasing magnetic field strengths (0 to 20 mT in 2 mT increments) while measuring the opening angles and testing their snap-opening behavior. In Fig. 3a, Design B ($4\times 2\times 4$ mm magnets, 1.30 mm spacing) emerged as the optimized design, achieving a clear snap-opening at approximately 10 mT, remaining closed until 9 mT. In contrast, Design A required 7.9 mT, and Design C needed 13.0 mT to achieve similar results. The results were recorded by captured images using the open-source Tracker software [23] and proved by the magnetic dipole models.

The study also highlighted the effects of magnet spacing, showing that too large a distance between magnets (Design D) caused the capsule to remain in an undesirable fully open state, while too small a spacing (Design E) required much higher magnetic fields to function effectively as shown in Fig. 3b. As a result, Design B demonstrated superior sealing and closing behavior, avoiding the folding-back issue encountered in other designs where the entire capsule is susceptible to complete collapse open. The optimized Design B not only opened consistently at lower magnetic fields but also achieved 83% of its maximum opening angle within just 2 mT of the last closed point. This was a significant improvement over the prior capsule, which only reached 35% of its maximum opening angle under the same conditions [5].

These findings from comprehensive understanding of trade-off among multiple optimization objectives (opening angles, sealing force, and closing torque) confirmed that Design B, with its optimized magnet size and positioning, is the most efficient and reliable choice for unambiguous snap-opening (angle of 144 degrees), making it a promising candidate for practical sampling applications.

B. Sampling Efficiency test

To evaluate the sampling efficiency, the percentage of obtained liquid sample weight per single actuation was compared against the weight of the empty capsule. The procedure involved first a measurement of the weight of the entirely empty capsule without any simulated digesta foods and liquid inside the sampling chamber. The capsule was then put into a stomach tissue of a swine model filled with simulated digesta liquid (a mix of hydrochloric acid and pulp orange juice) and actuated by the required magnetic field from the 8-coil electromagnetic system to generate the maximum opening torque based on a single actuation shown in Fig. 4. The actuation field is applied only once to maintain

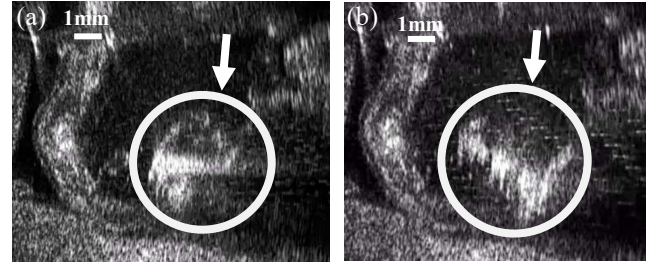


Fig. 4. Ultrasound image of the SOMAC capsule within the stomach tissue of a swine model in (a) closed state and (b) open state.

consistency between trials, as multiple actuations could result in increased sampling volume. The single actuation collected samples into the capsule's sampling chamber and then the volume of obtained samples was measured and analyzed. Five tests were performed, and the results were shown in Table II ($n=5$ capsules, with each capsule tested five times for all data points). The proposed design achieved an average of 67% (195 mg of samples out of 290 mg of fully obtained samples) and a maximum of 83% (239 mg of obtained samples) of the liquid sample volume obtained from a sampling chamber per single actuation. The surface tension occurring inside the small sampling reservoir would have generated these variations. Moreover, the SOMAC design significantly enhances the sampling volume ratio, utilizing more than half of the capsule's volume (53%, with a maximum reservoir capacity of 290 mg) for sampling purposes. In comparison, other magnetic hinge designs offer only 10% of its total volume as a sampling reservoir (Table I).

C. Capsule Sealing Test

This section evaluated the safe sample transit of the proposed capsule (SOMAC) in the GI tract, specifically focusing on its ability to withstand biological pressures during peristalsis. Gastric pressure is estimated at up to 10 kPa [19], and SOMAC was subjected to agitation tests that approximated 10 kPa. These tests involved agitating the capsules to assess its sealing properties and leakage potential. Fully loaded SOMAC capsules ($n = 3$), each containing 290 mg of simulated digesta and liquid, and unloaded capsules ($n = 3$) were placed in deionized water and agitated that exerted 10 kPa in a centrifuge (Sorvall Legend X1R; Thermo Scientific) at 300 rev/min for one hour at 25°C [5]. Following this, they were vortexed at 3000 rev/min for five minutes using an analog vortex mixer (VWR International, LLC) [5] ($n = 6$ capsules, with each capsule tested twice for all experimental results). The weight changes were recorded to determine any potential leakage or contamination. The results showed no significant differences in weight after agitation (an average of 1.6 mg and maximum of 2.6 mg), indicating that the sealing design effectively prevented any leakage under agitation.

We also analyzed the capsule's sealing forces, which play a critical role in its ability to secure larger samples. Different designs (A, B, C, and D) were tested, and the maximum sealing forces based on the dipole field gradient model shown in equation (3) were compared shown in Fig. 3c. Design B, which generated 2.8 N of force (experimentally measured at 2.8 ± 0.1 N), offered the most optimal sealing strength. The study highlighted that SOMAC's internal magnets, which are smaller

TABLE II. SAMPLING WEIGHT MEASUREMENTS OF SOMAC

Sampling Chamber Size	The proposed design (SOMAC): Maximum Volume of 290 mg				
	Sampling Weights (mg)				
Trials	1st Capsule	2nd Capsule	3rd Capsule	4th Capsule	5th Capsule
1st trial	216	157	171	222	192
2nd trial	153	169	198	204	226
3rd trial	203	175	192	238	175
4th trial	189	225	153	239	205
5th trial	132	235	212	169	219

in volume (32 mm³ of N50 magnets) compared to BCMAC (85 mm³ of N52 magnets) [5], produced a stronger sealing force. SOMAC's magnets were almost 2.7 times smaller in volume than BCMAC's but generated 3.7 times more sealing force. This stronger sealing force made SOMAC more efficient in handling larger samples, particularly in the upper GI tract, where the need for effective sealing is most critical. The sealing force was also found to significantly decrease as the distance between the internal magnets increased, which facilitated an unambiguous and clear snap-opening behaviors (see Fig. 3c). The clear opening behaviors of the capsule can be seen as the larger sealing force changes react sensitively to the small change in the distance between the two internal magnets. In conclusion, the sealing test demonstrated that SOMAC provides a reliable and effective means of collecting samples from the GI tract. Its design offers a stronger sealing force than comparable capsules, ensuring safe sample transit and clear operational performance, particularly in the early regions of the GI tract.

D. Biocompatibility Verification and Acid Resistivity

To ensure viability in the GI tract, specifically in a stomach environment, tensile analysis and acid resistivity of silicone rubber samples were conducted, the same as the material testing from Shokrollahi's paper [5]. The acid resilience test results for biocompatible properties in a stomach environment of the proposed design were analyzed stress-strain curves and an ultimate tensile strength for hydrochloric acid (HCl)-treated (n=5) and untreated (n=5) 20 wt% Part B silicone rubber samples. The t-test yielded a p-value of 0.17 between acid-exposed and unexposed samples, demonstrating no significant difference in tensile strength. Based on these results, it can be concluded that the proposed design's material properties maintain unaffected by the acidic conditions of the GI tract.

E. Locomotion and Sampling Test

This experiment verified the locomotion behavior of the capsule with a rotating external magnetic field. As the net magnetization direction of the internal magnets in the capsule is aligned along the external magnetic field verified in Section II and IV, the whole capsule body rotates, resulting in moving to a targeting area for sampling [24]. As the strength of the external magnetic field is critical to open the capsule for sampling or rotate for locomotion, the field magnitude less than the required field magnitude for opening would ensure that the capsule would be rotated while it is closed due to the unambiguous snap-open design. Therefore, the field magnitude for locomotion on Design B should be weaker than the 10 mT as shown in Fig. 3a and 3b. In all locomotion tests, rotating motion was conducted in a curved stomach model of a swine at a field magnitude of 3 mT and frequency of 1 Hz, completing locomotion and sampling in 1.5 minutes (Fig. 5b and 5c).

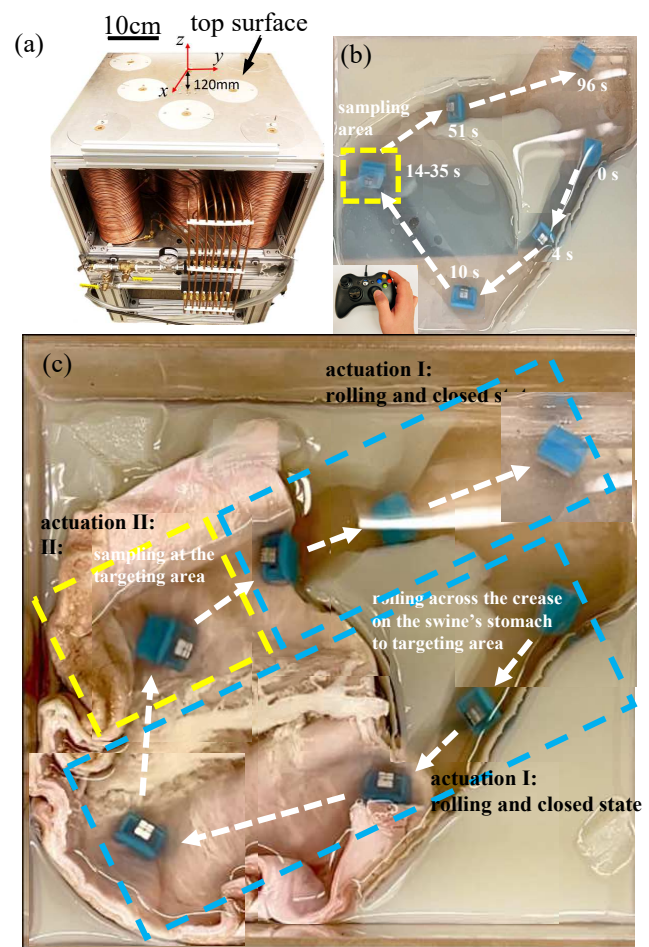


Fig. 5. (a) Actuation setup used for all experiments. A magnetic navigation system with eight electromagnets generates a uniform magnetic field strength over a substantial operating workspace, providing maximal workspace accessibility without constraints [24]. (b) Experimental setup for Design B, demonstrating rotating locomotion (3 mT, 1 Hz) and sampling in a phantom model made of agar gels, using an external rotating and uniform magnetic field. (c) SOMAC capsules rolling from their initial location to the target area along a curved stomach model of a swine for sampling, followed by retrieval. Snapshots from a top-view camera are shown.

V. CONCLUSION

The experimental results in Fig. 3 show excellent agreement with the model after they opened, but some results show only fair prediction around the critical region where capsules start to open due to fabrication error and the point dipole assumption. Overall, the proposed snap-open capsule (SOMAC) offers several advantages over previous designs. It features a higher volume ratio for sample collection due to more exposed surfaces and wider opening angles, improving sampling efficiency. The use of smaller magnets and thinner walls allows for more space in the collecting chambers. Additionally, its unambiguous snap-opening and stronger sealing properties ensure secure sample collection, while low magnetic fields enable operation at greater distances using smaller permanent magnets, proving a good potential under *ex vivo* sampling scenarios.

Despite these benefits, the capsule faced challenges with restoring torque, making it difficult to return to a closed state

after fully opening, as shown in Fig. 3b. With an 80% failure rate, we were able to confirm the experiment's results in too large a spacing between magnets (Design D), which remained in an undesirable fully open state (folding-back issue). This issue is caused by increased distance between inner magnets, reducing pulling force and closing torque [5]. One option to address this could be to include a stopper which limits the maximum opening angle, ensuring the capsule can close securely after activation. The stopper would also minimize stress and fatigue on the flexible hinge, preserving its durability under repeated actuations within a limited time and preventing the capsule from fully folding back or separating under strong magnetic fields. Further testing of the SOMAC in a live animal would further verify its robustness, reliability in collecting large samples, and would allow for a complete demonstration of the microbiome sampling process along the GI tract.

VI. ACKNOWLEDGMENT

We acknowledge Ann Ping for assistance with the ultrasound image processing.

VII. REFERENCES

- [1] M. J. Bull and N. T. Plummer, "Part 1: The Human Gut Microbiome in Health and Disease," *Integrative medicine (Encinitas, Calif.)*, vol. 13, no. 6, pp. 17-22., Dec. 2014.
- [2] S. Park, H. Lee, D.-i. Kim, H. Kee and S. Park, "Active Multiple-Sampling Capsule for Gut Microbiome,," *IEEE/ASME transactions on mechatronics*, vol. 27, no. 6, p. 4384-4395, Dec. 2022.
- [3] Z. Y. Kho and K. L. Sunil, "The Human Gut Microbiome - A Potential Controller of Wellness and Disease," *Frontiers in microbiology*, vol. 9, no. 9, Aug. 2018.
- [4] Y. P. Lai, T. Lee, D. Sieben, L. Gauthier, J. Nam and E. Diller, "Hybrid Hydrogel-Magnet Actuated Capsule for Automatic Gut Microbiome Sampling," *IEEE transactions on bio-medical engineering*, May 2024.
- [5] P. Shokrollahi, Y. P. Lai, S. Rash-Ahmadi, V. Stewart, M. Mohammadigheisar, L.-A. Huber, N. Matsuura, A. E. H. Zavodni, J. Parkinson and E. Diller, "Blindly Controlled Magnetically Actuated Capsule for Noninvasive Sampling of the Gastrointestinal Microbiome,," *IEEE/ASME Transactions on Mechatronics*, vol. 26, no. 5, pp. 2616-2628, Oct. 2021.
- [6] Y. Wang, J. Shen, S. H.-. Wang, M. Qiu, S. Du and B. Wang, "Microrobots for Targeted Delivery and Therapy in Digestive System,," *ACS Nano*, vol. 17, no. 1, p. 27-50, Dec. 2022.
- [7] M. Rehan, I. Al-Bahadly, D. G. Thomas, W. Young, L. K. Cheng and E. Avci, "Smart capsules for sensing and sampling the gut: status, challenges and prospects," *Gut*, vol. 73, no. 1, pp. 186-202, Dec. 2023.
- [8] L. Barducci, J. C. Norton, S. Sarker, S. Mohammed, R. Jones, P. Valdastrì and B. S. Terry, "Fundamentals of the gut for capsule engineers," *Progress in Biomedical Engineering*, vol. 2, no. 4, p. 042002, Sep. 2020.
- [9] S. Yim and M. Sitti, "Design and Rolling Locomotion of a Magnetically Actuated Soft Capsule Endoscope," *IEEE Transactions on Robotics*, vol. 28, no. 1, p. 183-194, Feb. 2012.
- [10] J. F. Waimin, S. Nejati, H. Jiang, J. Qiu, J. Wang, M. S. Verma and R. Rahimi, "Smart capsule for non-invasive sampling and studying of the gastrointestinal microbiome," *RSC Advances*, vol. 10, no. 28, p. 16313-16322, Apr. 2020.
- [11] M. B. Salem, G. Aiche, L. Rubbert, P. Renaud and Y. Haddab, "Design of a Microbiota Sampling Capsule using 3D-Printed Bistable Mechanism,," *2018 40th Annual International Conference of the IEEE Engineering in Medicine and Biology Society (EMBC)*, vol. 2018, pp. 4868-4871, 2018.
- [12] M. B. Salem, G. Aiche, Y. Haddab, L. Rubbert and P. Renaud, "Microbiota Sampling Capsule: Design, Prototyping and Assessment of a Sealing Solution Based on a Bistable Mechanism," *Journal of Medical Devices*, vol. 16, no. 4, p. 041009, Aug. 2022.
- [13] F. Munoz, G. Alici and W. Li, "A review of drug delivery systems for capsule endoscopy,," *Advanced Drug Delivery Reviews*, vol. 71, p. 77-85, May 2014.
- [14] J. Cui, X. Zheng, W. Hou, Y. Zhuang, X. Pi and J. Yang, "The study of a remote-controlled gastrointestinal drug delivery and sampling system," *Telemedicine journal and e-health : the official journal of the American Telemedicine Association*, vol. 14, no. 7, p. 715-719, 2008.
- [15] D. Becker, J. Zhang, T. Heimbach, R. C. Penland, C. Wanke, J. Shimizu and K. Kulmatycki, "Novel orally swallowable Intellicap® device to quantify regional drug absorption in human GI tract using Diltiazem as model drug," *AAPS PharmSciTech*, vol. 15, no. 6, p. 1490-1497, 2014.
- [16] M. Rehan, I. Al-Bahadly, D. G. Thomas and E. Avci, "Development of a robotic capsule for in vivo sampling of gut microbiota," *IEEE Robotics and Automation Letters*, vol. 7, no. 4, p. 9517-9524, Oct. 2022.
- [17] Y. Sun, W. Zhang, J. Gu, L. Xia, Y. Cao, X. Zhu, H. Wen, S. Ouyang, R. Liu, J. Li, Z. Jiang, D. Cheng, Y. Lv, X. Han, W. Qiu, K. Cai, E. Song, Q. Cao and L. Li, "Magnetically driven capsules with multimodal response and multifunctionality for biomedical applications," *Nature Communications*, vol. 15, no. 1, p. 1839, Feb. 2024.
- [18] L. Zheng, S. Guo and M. Kawanishi, "Magnetically Controlled Multifunctional Capsule Robot for Dual-Drug Delivery," *IEEE Systems Journal*, vol. 16, no. 4, pp. 6413-6424, Dec. 2022.
- [19] X. Liu, C. Steiger, S. Lin, G. A. Parada, J. Liu, H. F. Chan, H. Yuk, N. V. Phan, J. Collins, S. Tamang, G. Traverso and X. Zhao, "Ingestible hydrogel device," *Nature Communications*, vol. 10, no. 1, p. 493, Jan 2019.
- [20] S. Fujimori, "Gastric acid level of humans must decrease in the future," *World Journal of Gastroenterology*, vol. 26, no. 43, p. 6706-6709, Nov. 2020.
- [21] "Buy Clear Resin," Formlabs, 05 Jun 2024. [Online]. Available: <https://formlabs.com/store/materials/clear-resin-v4/>. [Accessed 09 Sep 2024].
- [22] "Mold Star™ 30 Product Information," Smooth-On, Inc., 2024. [Online]. Available: <https://www.smooth-on.com/products/mold-star-30/>. [Accessed 09 Sep 2024].
- [23] D. Brown, W. Christian and R. M. Hanson, "Tracker Video Analysis and Modeling Tool for Physics Education," Tracker, 2024. [Online]. Available: <https://physlets.org/tracker/>. [Accessed 09 Sep 2024].
- [24] A. Schonewille, C. He, C. Forbrigger, N. Wu, J. Drake, T. Looi and E. Diller, "Electromagnets Under the Table: an Unobtrusive Magnetic Navigation System for Microsurgery," *IEEE Transactions on Medical Robotics and Bionics*, vol. 6, no. 3, pp. 980-991, Aug. 2024.